Electrical Circuits with Chaotic Behavior

MARTIN J. HASLER, MEMBER, IEEE

Invited Paper

Several circuits that exhibit chaotic behavior are discussed. Evidence for such a behavior is given by laboratory experiments, by computer simulations, and, where available, by rigorous mathematical reasoning.

I. Introduction

The electrical engineer has been brought up with linear circuit theory. This is his reference when he thinks about circuits. The behavior of a nonlinear circuit is imagined as a distorted version of the behavior of a linear circuit. From this point of view, distortion of signals, generation of harmonics, etc., are an obvious consequence of the nonlinear characteristics of the circuit elements, and series expansions for the deviations from linear behavior is a natural tool to study these phenomena.

Such an approach is fully justified for weakly nonlinear circuits, but it is unable to describe the influence of strong nonlinearities. Moreover, it is impossible to draw the line between weak and strong nonlinearities just by looking at the circuit element characteristics. The interaction between different circuit elements is just as important.

The most spectacular manifestation of strong nonlinearity is the completely irregular behavior of very simple circuits whose nonlinear elements have perfectly regular characteristics. This type of phenomenon is generally called **chaotic behavior.** We will give a more precise meaning to this term in the sequel. Most electrical engineers are still unaware of this possibility and its occurrence may have been misinterpreted in many cases as some kind of external noise.

The purpose of this paper is to report on some of the evidence given for chaotic behavior of electrical circuits. The material can be divided into three categories:

a) laboratory experiments
b) computer simulations
c) mathematical proofs.

In science and technology as a whole, the literature reporting on chaotic phenomena is abundant. Unfortunately, mathematical proofs for the chaotic nature of satisfactory model systems are still rare. The field of electrical circuits is no exception.

In our opinion, completely convincing evidence for chaotic behavior is only given by a), b), and c) together. In fact, the chaotic behavior observed in the laboratory could be caused by some uncontrollable noise and the computer simulations could be strongly distorted by the accumulation of round-off errors. Mathematical proofs cannot be refuted as such, of course, but a case can be made that a mathematical model of a circuit might fail to reproduce the behavior of the physical circuit itself.

The electrical engineer is reluctant to accept the possibility of chaotic behavior because it is yet another effect that may cause a malfunctioning of the circuits he designs. To reassure him, nonlinear circuit theory should provide criteria that permit to single out the intervals for the design parameters, where chaotic behavior may occur. Unfortunately, at present this is only wishful thinking.

In the absence of a deeper understanding of the origin of chaos, one has to concentrate on the simplest circuits that show chaotic behavior. The minimum complexity is given by the Poincaré-Bendixon theorem which roughly says that the solutions of a system of two autonomous differential equations of first order converge either to a point or to a closed curve [1]. This excludes any permanent irregular behavior. Hence, in order to study chaos, one has to consider at least either **two nonautonomous equations** of first order, or **three autonomous equations** of first order. Translated into circuit language, this means that the presence of at least two reactive elements (capacitor, inductor) and a time-dependent source, or, alternatively, the presence of at least three reactive elements is required. This paper concentrates mainly on examples of the first type.

II. Asymptotic Behavior of the Solutions

When looking at the time evolution of the voltages and currents in a circuit, one usually distinguishes between the transient behavior, which disappears after a certain time and the permanent features which persist in time. The latter is referred to as the asymptotic behavior of the circuit, since permanent features of the time evolution have to be extracted in the limit as time goes to infinity. This does not mean that the transients need an infinitely long time to van-

Manuscript received December 5, 1986; revised January 14, 1987. This work was supported by the Swiss National Science Foundation under Grant 2.842-0.85.

The author is with the Department of Electrical Engineering, Swiss Federal Institute of Technology, 1015 Lausanne, Switzerland.

IEEE Log Number 8714769.

0018-9219/87/0800-1009$01.00 © 1987 IEEE

ish, but in this way one can study the permenant behavior without having to estimate the transient decay time first.

By chaotic behavior of a circuit, we mean an irregular asymptotic behavior. At this point, one remark is appropriate. There are examples of dynamic systems, where the solutions converge to an equilibrium point after a long transient period whose aspect is very irregular [2]. In computer simulations and in laboratory experiments such behavior would most probably be interpreted as permanently chaotic. This again shows the need for a rigorous mathematical analysis.

What is regular and what is chaotic asymptotic behavior? Let us consider a linear circuit excited by a sinusoidal voltage source. Each voltage and each current of the circuit, as a function of time, is a sum of terms generated by the initial charges and fluxes of the capacitors and inductors and a term generated by the time-dependent source. The natural frequencies of the circuit determine the qualitative behavior of the former and the time dependence of the source is reproduced by the latter. If the natural frequencies s_i are in the open left half of the complex s-plane (Re $s < 0$) then the former decay with exp $(-ts_i)$ and therefore constitute the transient part of the time evolution, whereas the latter is a sinusoid and constitutes the asymptotic behavior (Fig. 1).

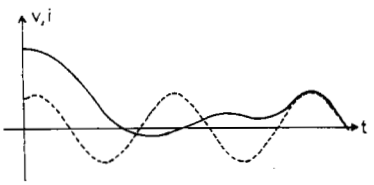

Fig. 1. Waveform of a linear circuit driven by a sinusoidal source.

Instead of studying the waveforms, i.e., the voltages and currents as functions of time, one often concentrates on the orbits in state space. The coordinates of the state space are the charges or voltages of the capacitors and the fluxes or the currents of the inductors. The time evolution of the circuit is represented, for each initial state, by a single curve in state space, the orbit. The time dependence is not visible anymore on the orbit, but the direction of increasing time can be indicated by arrows. In Fig. 2, an orbit belonging to a linear circuit with a capacitor C, an inductor L, resistors, and a sinusoidal voltage source is represented. The asymptotic orbit is an ellipse, corresponding to the sinusoidal steady state of the circuit. Note that for a different starting point the orbit would converge to the same ellipse.

If a linear circuit has constant sources in addition to the sinusoidal source, the time evolution of the voltages and the currents are up to a constant as well.

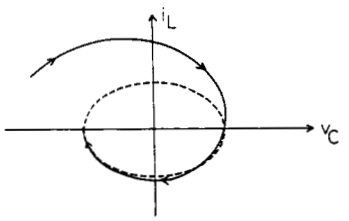

Fig. 2. State-space orbit of a linear circuit driven by a sinusoidal source.

The convergence of all waveforms to a unique sinusoidal steady state, the same for all possible initial states, is the most regular asymptotic behavior one can expect of a circuit with a sinusoidal source. If a linear circuit has a natural frequency in the open right half of the complex s-plane, all solutions diverge to infinity, with the exception of those where this natural frequency is not excited. Apart from the limiting cases, where the rightmost natural frequencies are on the imaginary axis, no other asymptotic behavior can occur in linear circuits.

The situation changes radically when nonlinear elements are admitted in the circuit. Apart from the "normal" behavior many qualitatively quite different time evolutions are possible [3]. Normal behavior means convergence of every voltage and current to a periodic function of time, which has the same period as the generator and is independent of the initial state. Figs. 1 and 2 give again a qualitative picture, except that the asymptotic waveform is in general not a sinusoid anymore and the asymptotic orbit not an ellipse.

A more complicated asymptotic behavior occurs when the circuit admits several different periodic time evolutions. Their periods may be the same as the period of the source, or multiples thereof (subharmonics). In general, some of them are stable, and others are unstable. The voltages and currents converge to one of the stable periodic time evolutions: which one depends on the initial state. The unstable periodic time evolutions are reached asymptotically only for exceptional initial states. Any other initial state, even very close to the exceptional ones, will converge to a different periodic steady state. For this reason, the unstable periodic time evolutions cannot be observed directly in laboratory experiments, and in computer simulations special algorithms have to be used. Note, however, that this kind of instability is different from the instability of a linear circuit mentioned above. There is no divergence to infinity. Note also that, apart from the exceptional initial states, the asymptotic behavior of the currents and voltages is the same for sufficiently close initial states.

In Fig. 3, an example with three periodic orbits is given.

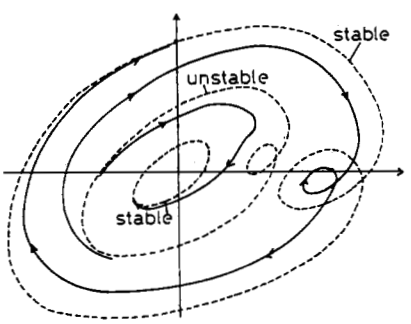

Fig. 3. Two state-space orbits of a nonlinear circuit with three periodic steady states.

Two of them are stable and one is unstable. Furthermore, two general orbits with different asymptotic behavior are represented.

Another possibility is the presence of an almost periodic steady state, i.e., a steady state containing frequencies that are not rationally related. In this case, the voltages and cur-

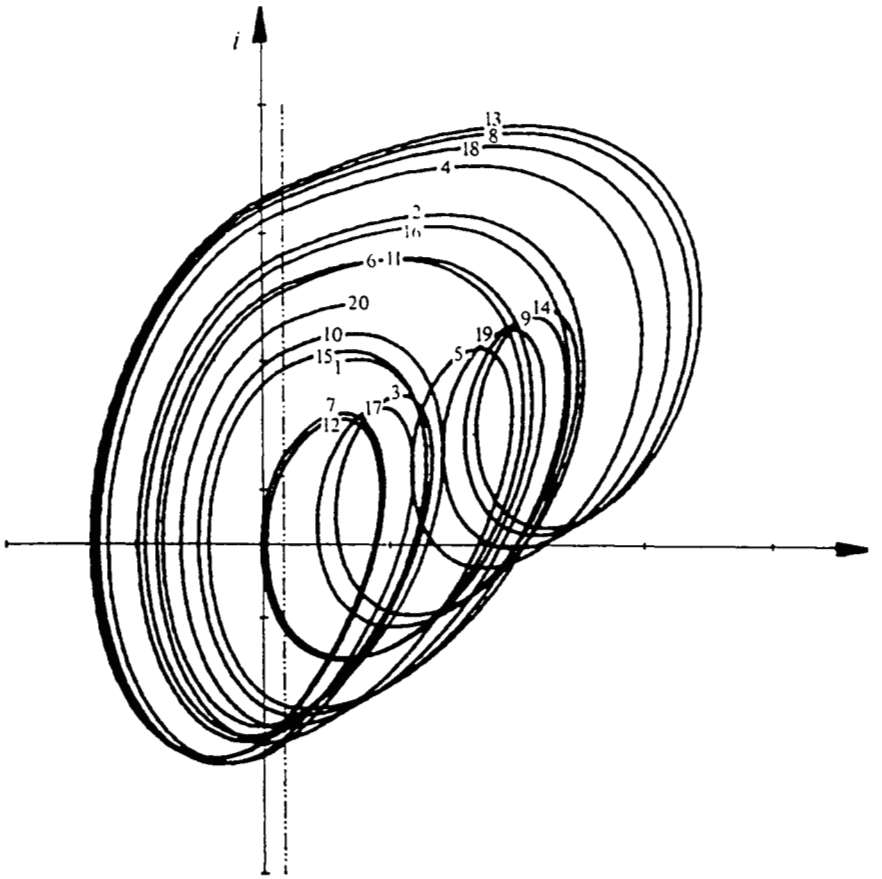

Fig. 4. Chaotic state-space orbit.

rents of the circuit look somewhat irregular for large periods of time, but different initial states still lead to the same asymptotic functions of time. Furthermore, these functions are nearly periodic with large periods.

The asymptotic behavior may be worse still. It may even fail to be approximately periodic. The orbits in state space appear to fill out whole regions (Fig. 4). Furthermore, close initial states lead to time evolutions that become more and more distant from each other. Thus all time evolutions are unstable. **This is chaotic behavior.**

III. The Forced van der Pol Oscillator

The circuit of Fig. 5 is known as the forced van der Pol oscillator, if the nonlinear resistor has the characteristic

$$f(i) = Ri_0(-i/i_0 + (i/i_0)^3/3) \tag{3.1}$$

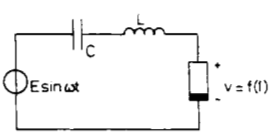

Fig. 5. Forced van der Pol oscillator.

where i_0 and R are a normalization current and a normalization resistance, respectively (Fig. 6). The solutions of this circuit satisfy the second-order differential equation

$$\epsilon d^2x/dt^2 + \phi(x)\, dx/dt + \epsilon x = b \cos(\omega t) \tag{3.2}$$

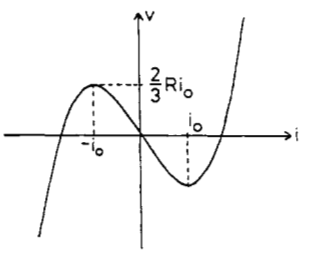

Fig. 6. Characteristic of the nonlinear resistor in the van der Pol oscillator.

where the following normalizations have been used: $\epsilon = \sqrt{L/(CR^2)}$, $\phi = f'/R$, $t \to \sqrt{LC}\, t$, $\omega \to \omega/\sqrt{LC}$, $b = E\omega/(\sqrt{LC}\, R)$, and $x = i/i_0$.

As early as 1945, Cartwright and Littlewood have discovered that (3.2) has, at least for small ϵ, "bad" solutions [4]. The detailed proofs are given in [5]. Levinson [6] provided a simpler proof for this "singular behavior" in 1949, by replacing the characteristic of Fig. 6 with the piecewise-linear characteristic of Fig. 7.

The paper of Levinson has deeply influenced the subsequent development of mathematical analysis. Indeed, it has been the starting point for Smale to construct his famous "horseshoe" example, which is one of the prototypes for chaotic behavior [7]. Equipped with modern mathematical theory the origin of which was the paper of Smale, Levi [8] has reconsidered the forced van der Pol oscillator, with a nonlinear resistor characteristic as in Fig. 6, but whose cor-

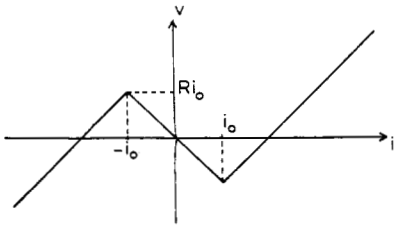

Fig. 7. Piecewise-linear resistor characteristic considered by Levinson.

ners have been rounded off and with a modified periodic source.

We sketch here the arguments of Levinson. The circuit of Fig. 5 with the nonlinear resistor characteristic of Fig. 7 is piecewise linear. This means that the space of the voltages and currents is subdivided into a number of regions, three in our example, within which the circuit behaves exactly like a linear circuit. The nonlinearity of the overall circuit originates from the switching from one linear circuit to another when the voltages and currents pass the boundary of a linear region.

On the x-axis the linear regions are the intervals $(-\infty, -1]$, $[-1, +1]$, $[+1, +\infty)$. In the central interval, the function ϕ is the constant -1, and in the left and right intervals it is the constant $+1$. Consequently, the linear circuit corresponding to the central interval is unstable and the linear circuits corresponding to the outside intervals are stable.

The natural frequencies for the region $|x| \leqslant$ are

$$\rho = (1 - \sqrt{1 - 4\epsilon^2})/2\epsilon \simeq \epsilon \tag{3.3}$$

and $1/\rho$. Thus the solutions of (3.2) in this region are of the form

$$x(t) = B_1 \exp (t - t_0)/\rho + B_2 \exp (t - t_0)\rho + (b/\omega) \cos (\omega t). \tag{3.4}$$

The first exponential term in (3.4) grows very fast and thus the solutions of (3.2) cross this linear region very rapidly (Fig. 8), unless the coefficient B_1 is very small which implies a certain delay for the crossing of the region.

In the two linear regions with $|x| \geqslant 1$, the natural frequencies are $-\rho$ and $-1/\rho$ and the solutions have the form

$$x(t) = A_1 \exp -(t - t_0)/\rho + A_2 \exp -(t - t_0)\rho - (b/\omega) \cos (\omega t). \tag{3.5}$$

The first term vanishes very rapidly and the remaining two terms constitute a slowly decreasing exponential that is modulated by a cosine.

The method of Levinson consists in considering simultaneously a whole set of solutions. Each solution is identified by the instant t_0 at which it crosses the boundary $x = -1$ and the derivative dx/dt at t_0. The family F of solutions considered by Levinson have their crossing points on an arc C in the shaded doman Z of the $(\omega t_0 \cdot \dot{x}_0)$-plane, as shown in Fig. 9. For the exact definition of Z and the kind of arc that is admitted we refer to [6].

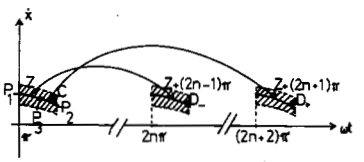

Fig. 9. Family F of solutions on the boundaries $x = -1$ and $x = 1$.

The two solutions of (3.2) that correspond to the two endpoints P_1 and P_2 of C are represented in Fig. 8 as functions of time. Note that both grow to a maximum of approximately $x = 3$ and then decrease slowly. The solution that crosses the central region first re-enters this region shortly after $\omega t = 2n\pi$ whereas the other has to wait another period of the modulating cosine and re-enters $|x| \leqslant 1$ shortly after $\omega t = (2n + 2)\pi$. The integer n depends on the value of ρ; the smaller is ρ, the larger is n.

Consider now the whole family F, not only the endpoints of the arc. There must be a point P_3 on the C, whose solution touches the boundary $x = 1$ shortly after $\omega t = 2n\pi$, but that enters the central region only after $\omega t = (2n + 2)\pi$. It is shown in [6] that all solutions corresponding to the portion

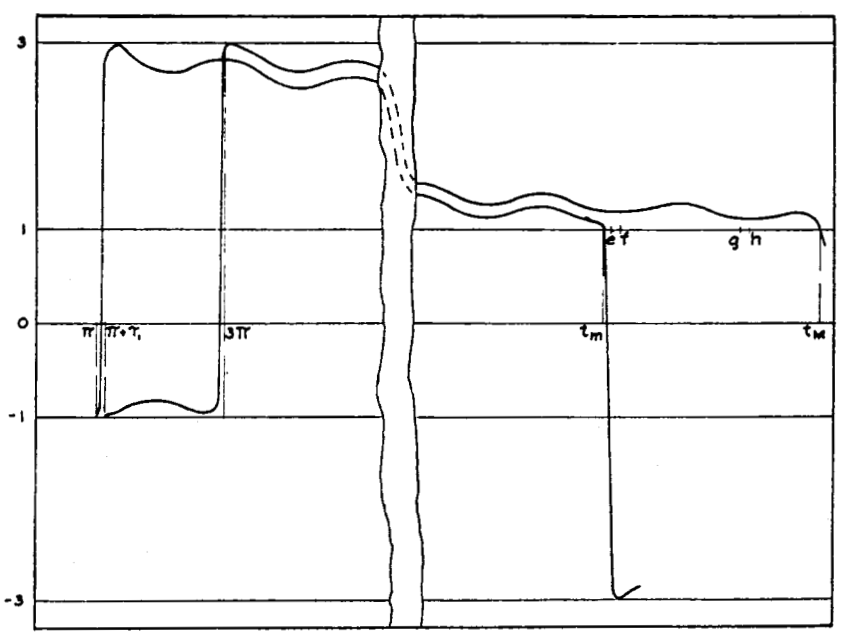

Fig. 8. Two solutions of (3.2) (from [6]).

C_- from P_1 to P_3 of the arc enter the central region shortly after $\omega t = 2n\pi$. Furthermore, if for each solution we observe the time t_1 when it crosses the boundary $x = 1$ and the derivative dx/dt, and if we represent it as a point in the plane $(\omega t_1 \cdot \dot{x}_1)$, then we get a curve D_- of the same kind as C, in the domain $Z + (2n - 1)\pi$. Similarly, the solutions starting from the arc C_+, whose endpoints are P_3 and P_2 on $x = -1$ cross $x = +1$ on an arc D_+ of the same kind as C.

To sum up, following the solutions from the boundary $x = -1$ until they re-enter the region $|x| \leqslant 1$ through the boundary $x = +1$ amounts to stretching the arc C, dividing it into two pieces, translating it along the time axis by $(2n - 1)\pi$ and $(2n + 1)\pi$, respectively, to end up with two arcs D_+ and D_- that are similar to C (Fig. 9). If we continue to track the solutions until they re-enter the central region through the boundary $x = -1$, the arcs D_- and D_+ split into four arcs E_{--}, E_{-+}, E_{+-}, and E_{++}, all similar to C, that lie in the domains $Z + (4n - 2)\pi$, $Z + 4n\pi$, and $Z + (4n + 2)\pi$.

Repeating this reasoning, Levinson showed that for each sequence δ_k of numbers $+1$ and -1, there is a solution of (3.2) that starts from the arc C and whose successive entry times of the region $|x| \leqslant 1$ are separated by approximately the quantity $(2n + \delta_k)\pi/\omega$.

For periodic sequences δ_k. Levinson proves that there exists a corresponding periodic solution. Thus there are periodic solutions of all periods that are linear combinations of $(2n - 1)\pi/\omega$ and $(2n + 1)\pi/\omega$ with natural numbers as coefficients. Equation (3.2) thus has an infinity of periodic solutions. They are all unstable.

However, most of the sequences δ_k are not periodic, not even asymptotically periodic and the corresponding solutions therefore have no periodic asymptotic behavior. This, together with [5], is the first proof for irregular asymptotic behavior of the solutions of ordinary differential equations.

So far, the mathematical evidence for the chaotic behavior of the forced van der Pol oscillator was given. How about computer simulations and laboratory experiments? Parker and Chua reported in [9] on a large number of computer simulations on the piecewise-linear circuit whose equations Levinson has studied. They varied the parameters ϵ and b of (3.2) and noted the asymptotic behavior for each pair of parameters. Keeping ϵ fixed at a small value and varying b, they found stable periodic solutions of all periods that are odd multiples of $2\pi/\omega$. For a given value of b, either a single stable subharmonic of period $(2n + 1)\pi$ is present, or two of them coexist, with periods $(2n - 1)\pi$ and $(2n + 1)\pi$. This is not in contradiction with the work of Levinson. In fact, studying a set of solutions starting from an arc different from C, he could prove the existence of these subharmonics for most values of b.

But where are the chaotic solutions? Parker and Chua could not find them by computer simulation. The analysis of Levi shows that in the space of initial conditions they form a set of measure zero, i.e., an infinitely thin set. Therefore, it is hopeless to find them in laboratory experiments, and special algorithms would have to be devised to compute them numerically. However, it is not difficult to explain their presence intuitively. In fact, they always occur when there are simultaneously two stable subharmonics of different periods. They are located exactly between the domains of attraction of the two subharmonics. Indeed, for some time they adopt one of the periods, then the other, then they go back for some time to the first period, etc. The whole pattern is perfectly arbitrary. It is given for each chaotic solution by the aperiodic sequence δ_k.

IV. Other Forced Oscillators

It is very likely that chaotic behavior has frequently been observed in laboratory experiments, but that these observations have been misinterpreted as failures of the measuring equipment, as parasitic noise, etc. Reporting on such "unsuccessul" experiments does not add much to the reputation of the experimenter and thus it is unlikely to find any records of them in the literature.

A remarkable exception is the paper of van der Pol and van der Mark [10] that appeared as early as 1927. They studied the neon tube oscillator of Fig. 10 that is excited by a sinusoidal and a constant voltage source. The neon bulb

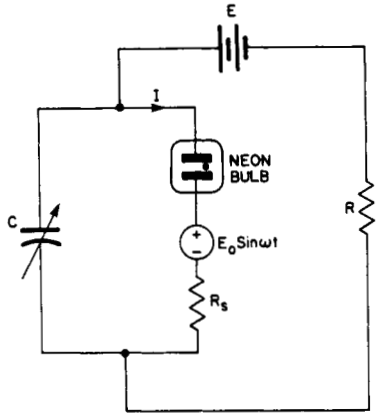

Fig. 10. Forced neon bulb oscillator (from [11]).

can be modeled by a linear inductor in series with a nonlinear resistor whose characteristic is given in Fig. 11. The purpose of this circuit was to generate subharmonics. In order to observe the fundamental frequency, van der Pol and van der Mark simply coupled a telephone receiver in some way loosely to the circuit and listened to it!

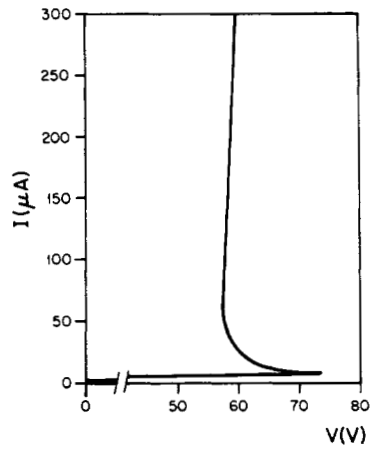

Fig. 11. Neon bulb characteristic (from [11]).

When the amplitude of the sinusoidal source E_0 is zero, the circuit oscillates at a certain frequency ω_0. By varying the capacitor C, van der Pol and van der Mark have covered a whole frequency interval for ω_0. In the presence of the sinusoidal source of frequency ω, they have observed the following phenomena. If ω_0 was sufficiently close to ω, the circuit oscillated at frequency ω. Lowering ω_0 continuously, at a certain point the synchronization between the oscil-

lator circuit and the sinusoidal source was lost. Later on, the oscillator locked onto the frequency $\omega/2$. Continuing to lower ω_0, the oscillator lost synchronization with the subharmonic 1/2, as well, and, as soon as ω_0 was sufficiently close to $\omega/3$, this frequency would be forced onto the oscillator. This process continued as the neon bulb circuit successively passed through the subharmonics 1/2, 1/3, 1/4, etc.

This behavior was what the two authors were looking for. However, between the frequency where the synchronization with one subharmonic was lost and the frequency where the oscillator was locked to the next frequency, there was an interval where they observed "irregular noise." We know now that they have listened to chaos.

Strangely enough, the forced van der Pol oscillator, where chaos is not observable, has led to extensive studies of chaotic systems, whereas the neon bulb oscillator has long been forgotten, even though chaos has been observed using only primitive measuring equipment. The experiments of van der Pol and van der Mark have recently been taken up by Kennedy and Chua with more sophisticated measuring apparatus [11]. They have found in the transition intervals a complicated succession of subharmonic and chaotic behavior.

Similar phenomena have been observed by Pei, Guo, Wu, and Chua [12], and Chua, Yao, and Yang [13] in other forced negative resistance oscillators, where the nonlinear resistor is implemented by two bipolar transistors. We briefly present the results of [13], because they are particularly appealing. The circuit is represented in Fig. 12, the implementation of the nonlinear resistor in Fig. 13, and its characteristic in Fig. 14.

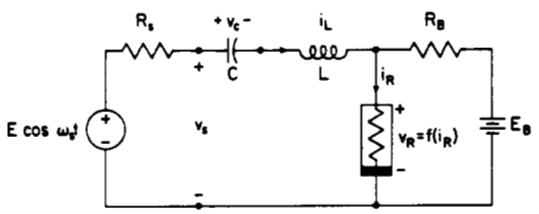

Fig. 12. Forced negative resistance oscillator (from [13]).

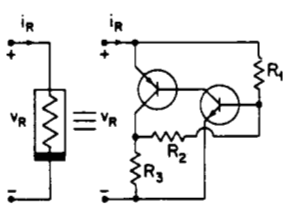

Fig. 13. Implementation of the nonlinear resistor (from [13]).

Fig. 14. Nonlinear resistor characteristic (from [13]).

Instead of changing the frequency of the unforced oscillator, the forcing frequency f_s is varied. In Fig. 15, the ratio P of f_s and the fundamental frequency of the forced oscillator is represented as a function of f_s. Thus $P = m$ corresponds to a subharmonic $1/m$. The synchronization intervals with $P = 1, 2, 3$, etc., are clearly visible, as well as the gaps between these intervals where the details are omitted. In Fig. 16, the gap between the $P = 1$ and $P = 2$ is enlarged.

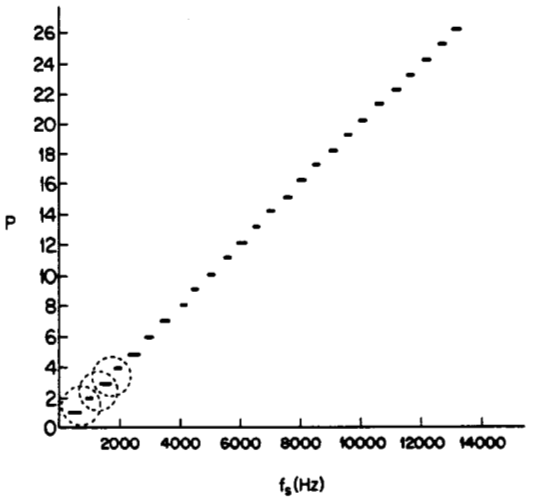

Fig. 15. Main sequence of subharmonics (from [13]).

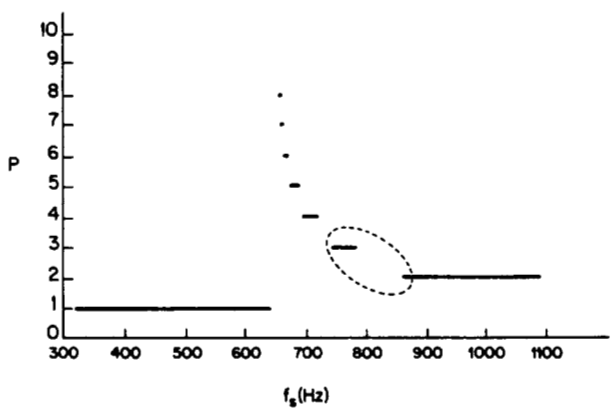

Fig. 16. Secondary sequence of subharmonics in the first gap of Fig. 15 (from [13]).

A secondary sequence of subharmonics with $P = 3, 4, 5$, etc., fills this gap partially. Only partially, because on the one hand there are again gaps between these secondary intervals and on the other hand, the left limit of the secondary sequence of subharmonics lies to the right of the right-hand limit of the primary interval $P = 1$. Indeed, for the frequencies in between, chaotic behavior is observed. In Fig. 17, the orbit of the 1/4 subharmonic belonging to this secondary sequence is represented in the (v_s, v_c)-plane, whereas in Fig. 18 the orbit of the chaotic regime to the left of the secondary sequence is shown.

In the other gaps of the primary sequence of synchronization intervals the same phenomenon takes place, except that P does not increase by 1 in the secondary sequence of gap n, but by steps of n.

Furthermore, in the gaps of the secondary sequences there appears a third sequence of subharmonics. In Fig. 19,

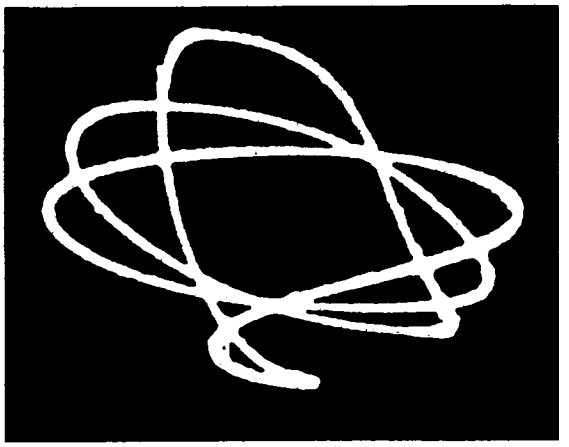

Fig. 17. Orbit of the subharmonic 1/4 belonging to the secondary sequence of Fig. 16 (from [13]).

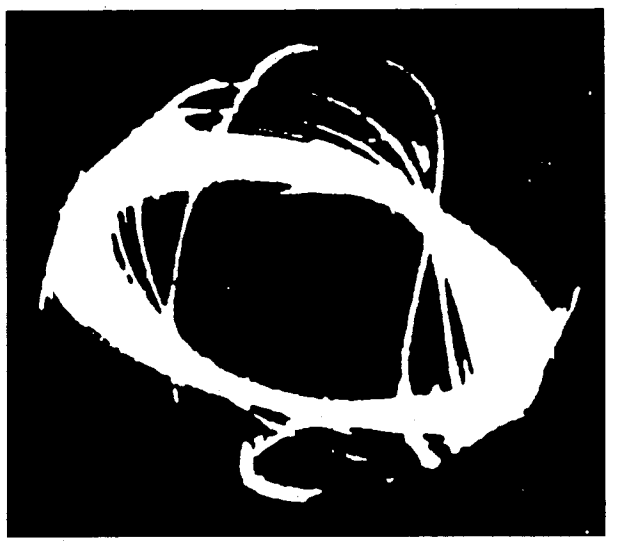

Fig. 18. Orbit of the chaotic regime beyond the secondary sequence of Fig. 16 (from [13]).

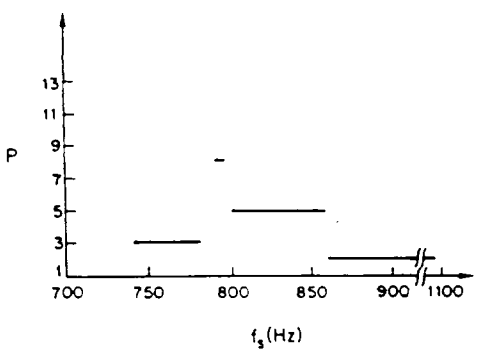

Fig. 19. Third-order sequence of subharmonics in the first gap of the secondary sequence of Fig. 16 (from [13]).

the first gap of the first secondary sequence is enlarged. The subharmonics with $P = 5$ and $P = 8$ are clearly visible in the gap bordered by the $P = 2$ and $P = 3$ subharmonics of the secondary sequence. To climb up further on the third sequence is beyond the reach of the measuring apparatus.

From their observations, Chua, Yao, and Yang conjectured the following general picture: There is a whole hierarchy of sequences of subharmonics. The corresponding sequences of P-values increase by constant increments to infinity, like staircases. Except for the main sequence, the width of the steps decreases to zero. The authors have used the term "devil's staircase." Furthermore, there are gaps between the steps of the staircases. The gaps of an nth-order staircase is partially filled with a staircase of order $n + 1$. The filling is only partial, because between the steps of this staircase there are again gaps and beyond the staircase there is chaos. Chua, Yao, and Yang were able to give simple laws for the sequences of P-values for all staircases.

This beautiful pattern of finer staircases, one contained in the other, is an example of a geometric object that looks similar at different scales. Such objects are called "fractals" and have been advocated by Mandelbrot [14].

Returning to the forced van der Pol oscillator, it is sufficient to add a nonlinear term in (3.2) to obtain observable chaotic behavior. The equation

$$d^2x/dt^2 + \mu(x^2 - 1)\, dx/dt + x^3 = B \cos(\nu t) \qquad (4.1)$$

has been studied by Ueda, Akamatsu, Kawakami, and Hayashi [15], [16]. It is known under the name of "Duffing-van der Pol equation."

V. Loss of Synchronization

The appearance of chaos in the examples that have been discussed so far can be explained by a loss of synchronization between the unforced oscillator and the forcing generator. While this interpretation is very plausible, it should be confirmed by some mathematical argument to become convincing. The work of Levinson is a step in this direction. For the other examples cited above, to the knowledge of the author, nothing rigorous is available. There is another circuit, however, where precisely the mechanism of synchronization loss is studied.

According to Tang, Mees, and Chua [17], the forced astable multivibrator of Fig. 20 is a good model for many oscillators that are frequency-stablized by a reference signal. It contains a piecewise-linear resistor with the characteristic of Fig. 21 and it is excited by the small synchronization signal of Fig. 22.

The circuit of Fig. 20 has two impasse points [3] that are labeled C and B in Fig. 21. Small parasitic elements will cause the time evolution to jump from point C to point A and from

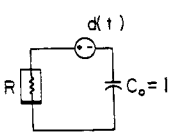

Fig. 20. Forced astable multivibrator (from [17]).

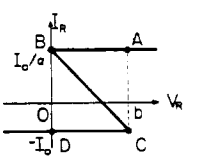

Fig. 21. Piecewise-linear resistor characteristic (from [17]).

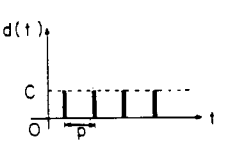

Fig. 22. Synchronization signal (from [17]).

point B to point D. Hence, in the absence of the signal $d(t)$, the capacitor is charged by the resistor during the time b/I_0 needed to pass from point D to point C, and then discharges onto the resistor during the time $b\alpha/I_0$ needed to pass from point A to point B. The presence of the signal $d(t)$ may trigger the jump from C to A before the capacitor voltage has reached the threshold b. This occurs if a pulse arrives when the capacitor voltage is rising between the values $b - c$ and b. Otherwise, the pulses have no effect.

If the period p of the signal is slightly smaller than the period q of the free-running multivibrator, all pulses will trigger the jump and thus the forced multivibrator is synchronized with $d(t)$. This is the normal functioning of the frequency-stabilized oscillator (Fig. 23). However, if p is

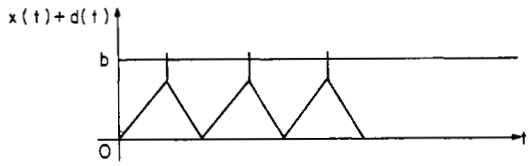

Fig. 23. Waveform of the synchronized oscillator (from [17]).

slightly larger than q, there is a certain number k of pulses which will not trigger a jump between two triggering pulses (Fig. 24). Using the notation of Fig. 24, we get

$$t_{n+1} = (p - q)k - \alpha t_n. \tag{5.1}$$

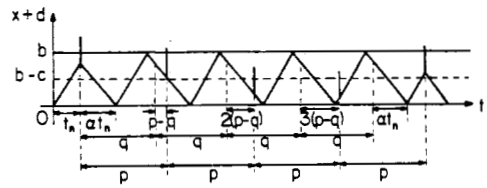

Fig. 24. Waveform of the oscillator when synchronization is lost (from [17]).

On the other hand, the time for the capacitor to be charged from zero to the triggering threshold voltage $b - c$ is $(b - c)/I_0$. Therefore

$$(p - q)(k - 1) < \alpha t_n + (b - c)/I_0 \leq (p - q)k \tag{5.2}$$

which can be rewritten as

$$\alpha t_n + (b - c)/I_0 = (p - q)(k - 1) + (\alpha t_n + (b - c)/I_0) \bmod (p - q). \tag{5.3}$$

Eliminating k between (5.1) and (5.3) we get

$$t_{n+1} = (p - q) + (b - c)/I_0 - (\alpha t_n + (b - c)/I_0) \bmod (p - q). \tag{5.4}$$

This equation is of the form

$$\tau_{n+1} = f(\tau_n) = 1 - (\alpha\tau_n + \beta) \bmod (1) \tag{5.5}$$

where

$$\tau_n = (t_n - (b - c)/I_0)/(p - q) \tag{5.6}$$

$$\beta = (b - c)(1 + \alpha)/(p - q)I_0. \tag{5.7}$$

To each time evolution of the circuit there corresponds the sequence τ_n, which is obtained by iterating the function f on the initial value τ_0. The function f is represented in Fig. 25. It is composed of two continuous branches. Each branch

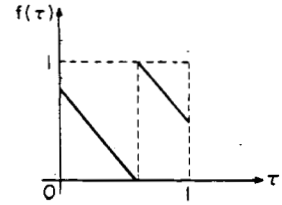

Fig. 25. The function defined in (5.5) (from [17]).

corresponds to a different number k of free-running oscillations of the multivibrator between two triggering pulses. It is not difficult to analyze the iterations of f rigorously. The results of this analysis are as follows:

In the **case $\alpha < 1$** all sequences τ_n converge to a fixed point of f. This corresponds to a stable subharmonic regime of the forced oscillator.

In the **case $\alpha > 1$,** no periodic sequence τ_n can be stable. Furthermore, each almost periodic sequence is in fact periodic. This shows that, apart from exceptional initial conditions, the asymptotic behavior of the forced oscillator is never periodic, nor almost periodic. In terms of frequency content, the Fourier transform of the voltage and current waveforms is never composed uniquely of rays, it always has a continuous part. A typical Fourier transform is represented in Fig. 26.

Another manifestation of the chaotic behavior in the case $\alpha > 1$ is the **sensitive dependence on initial conditions.** Since $d\tau_{n+1} = -\alpha d\tau_n$, sequences with very close initial τ_0's diverge from each other with exponential speed $\ln \alpha$ until they are on different branches of f. This means that all sequences are unstable. Even microscopically close initial conditions will lead eventually to macroscopically different sequences.

To sum up, the chaotic nature of the time evolution has been proved rigorously for the circuit of Fig. 20, when the reference signal has a slightly lower frequency than the free-running astable multivibrator. Both the irregular nature of the asymptotic behavior and the sensitive dependence on initial conditions have been put on firm grounds. However, there is no discussion on the loss of synchronization when the frequency of the reference signal is too high with respect to the free-running frequency of the multivibrator.

Another remark is appropriate. The circuit of Fig. 20 has only one reactive element, the capacitor. Since a nonautonomous first-order differential equation can be transformed into a system of two first-order autonomous differential equations, the chaotic nature of its solutions seems to be in contradiction with the Poincaré-Bendixon theorem [1]. Remember, however, that there were two impasse points and that we have introduced a jump rule to be able to continue the time evolution from the impasse points. In fact, this procedure is justified by noting that such discontinuous waveforms are obtained in the limit when certain parasitic reactances tend to zero. Thus we actually consider a circuit with at least two reactances, the capacitor and a parasitic inductor, and the Poincaré-Bendixon theorem does not apply anymore.

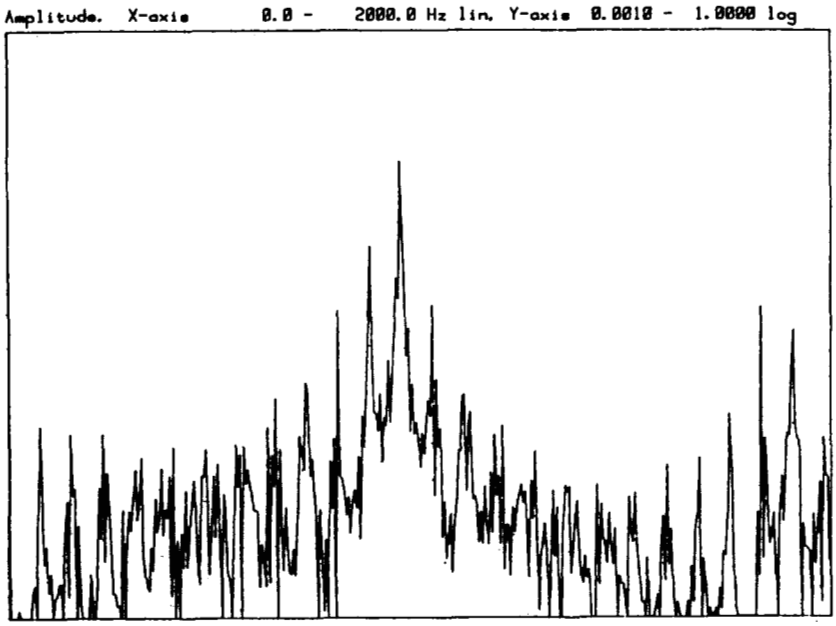

Fig. 26. Spectrum of a typical waveform of v_c (from [17]).

VI. *R-L*-Diode Circuit

The circuit of Fig. 27 does not fall into the class of forced oscillators. Indeed, if the voltage source is set to zero, all voltages and currents of the circuit converge to zero, irrespective of the initial conditions. This property is a con-

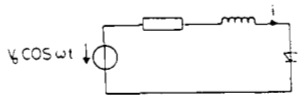

Fig. 27. *R-L*-diode circuit.

sequence of the passivity of the circuit elements. It can be proved by using the stored energy as a Liapunov function [3]. Therefore, it does not make sense to talk about synchronization in this case.

Testa, Perez, and Jeffries [18] have observed by laboratory experiments that this circuit may have a complicated asymptotic behavior. In Fig. 28, the bifurcation diagram is represented that they have directly obtained on the oscilloscope. This picture is to be interpreted as follows. The horizontal axis represents the source amplitude V_0 and the vertical axis the diode voltage v. For each value of V_0, the diode voltages $v(t_0 + nT)$, for $n = N, N + 1, \cdots$ are plotted,

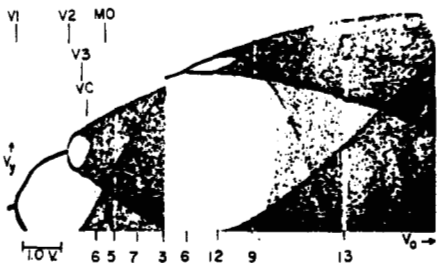

Fig. 28. Bifurcation diagram from the oscilloscope (from [18]).

where T is the source period, t_0 a constant time between 0 and T, and N a sufficiently large number such that the transient part of the time evolution has vanished at time NT. Hence, Fig. 28 gives a global picture of the asymptotic behavior of the *R-L*-diode circuit as a function of source amplitude V_0.

A priori, on the vertical line corresponding to a fixed amplitude V_0, a huge number of different points could be present. This actually is the case for certain portions of the bifurcation diagram, but not for others. Indeed, for small V_0, all points are superposed, which means that the values of $v(t_0 + nT)$ coincide and that $v(t)$ is asymptotically periodic of period T. This is the "normal" behavior of the circuit. The line of the points $v(t_0 + nT)$ suddenly bifurcates into two lines at a certain amplitude $V1$. This means that the voltages $v(t_0 + nT)$ oscillate between two values and that the $v(t)$ is asymptotically periodic of period $2T$. In other words, the voltages and currents of the circuit tend to a subharmonic 1/2 for these values of V_0. There follows a bifurcation at $V2$ to a subharmonic 1/4, and a bifurcation at $V3$ to a subharmonic 1/8. The resolution of the measuring apparatus comes to a limit, but by extrapolation one expects progressively shorter intervals of V_0 to follow, corresponding to the subharmonics 1/16, 1/32, etc. Indeed, convergence of the bifurcation points on the V_0-axis to a value V_c is conjectured. Beyond this amplitude, all voltages $v(t_0 + nT)$ are different which corresponds to chaotic behavior. Within the region of chaos, "windows" with series of subharmonics can be observed. The largest window in Fig. 28 is filled with the succession of subharmonics 1/3, 1/6, 1/12, etc.

It is interesting to compare this "route to chaos" with the route of Fig. 16. In Fig. 28, the subharmonics continue to double their period until chaos is reached, whereas in Fig. 12 constant increments are added.

If the circuit of Fig. 27 is to be simulated on a computer, a model has to be chosen for the diode. The most popular model is a nonlinear resistor with an exponential characteristic. It can be shown [3] that the resulting circuit behaves "normally" for any source amplitude V_0. Consequently, this

diode model cannot explain the bifurcation diagram of Fig. 28. Even if a linear capacitor is added in parallel, no complicated dynamics can occur [3]. A nonlinear junction capacitor in parallel with the nonlinear resistor is essential for generating subharmonics and chaos.

In [19], Azzouz, Duhr, and Hasler have simulated the circuit of Fig. 27 by using the standard SPICE program. The built-in diode model is composed of an exponential resistor and a capacitor that has a fractional power characteristic in the blocked mode and an exponential characteristic in the conducting mode. The results of the simulation are represented in a bifurcation diagram (Fig. 29) similar to Fig. 28, except that the inductor currents $i(t_0 + nT)$, $n = 1000, \cdots, 1029$, are plotted instead of the diode voltage. Note the good agreement between Figs. 28 and 29.

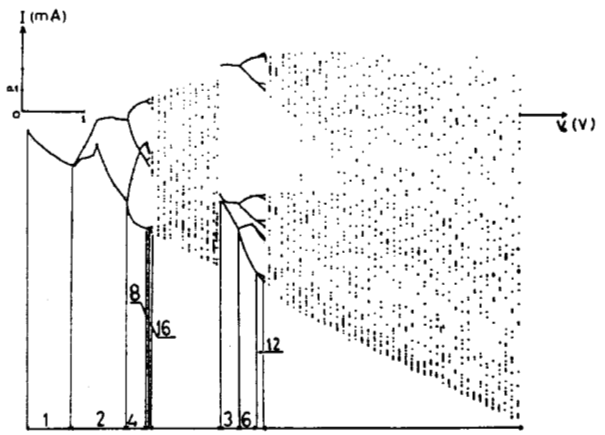

Fig. 29. Bifurcation diagram computed by SPICE (from [19]).

In order to accelerate the computations and also with the idea of an easier theoretical approach in mind, Azzouz, Duhr, and Hasler have drastically simplified the diode model in [20]. They have chosen a piecewise-linear characteristic for both the nonlinear resistor (Fig. 30) and the nonlinear capacitor (Fig. 31). Both characteristics have only two linear regions, with the same breakpoint, corresponding to the blocked and the conducting state of the diode. The resulting bifurcation diagram (Fig. 32) is surprisingly

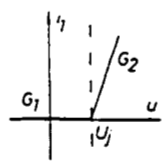

Fig. 30. Piecewise-linear resistor characteristic for the diode (from [20]).

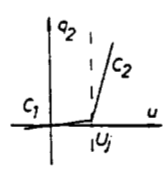

Fig. 31. Piecewise-linear capacitor characteristic for the diode (from [20]).

similar to Figs. 28 and 29. This shows that the qualitative aspects of the time evolution, and in particular the presence of chaos, does not depend on the particular form of the element characteristics. They are **robust phenomena.**

Is it possible to further simplify the circuit without destroying its complicated dynamic behavior? It is. In [21], Matsumoto, Chua, and Tanaka have eliminated the resistor in the diode model. Hence, their only nonlinear element is a piecewise-linear capacitor with the characteristic of Fig. 31. The resulting bifurcation diagram (Fig. 33) does not differ much from the others. This still confirms the robustness of chaos.

The route to chaos through a period doubling sequence of subharmonics has been studied rigorously in the context of functions that map the interval $[-1, +1]$ into itself and that have a maximum at 0 [22], e.g.,

$$f(x) = 1 - \mu x^2. \tag{6.1}$$

A variant of (6.1) is widely known under the name of "logistic equation." Starting from an initial value x, the asymptotic properties of the iterates of f, $f(x)$, $f(f(x))$, $f(f(f(x)))$, etc., are studied as a function of μ. Again, a bifurcation diagram is obtained by plotting, for each value of μ, the nth iterates of f, for $n = N, N + 1, \cdots$ (Fig. 34). Apart from a few details, this completely different dynamical system produces the same bifurcation diagram! This fact suggests the idea to link the R-L-diode circuit in some way to the iterates of functions on the interval, in order to profit from the rigorous results of [22]. Yoon, Song, Shin, and Ra [23] used such an approach, but it lacks rigor and thus does not lead to any new proofs.

VII. Other Nonautonomous Circuits

There are other nonautonomous circuits with chaotic behavior, in particular the circuits that are described by the Duffing equation [24]. In [25], Melnikov's method is used to prove the presence of chaotic behavior. This is a perturbation method and thus presupposes that certain parameters are small. The same method has been applied in [26] to a Josephson-junction circuit.

A piecewise-linear circuit that models high-voltage equipment has been studied in [27] and chaotic behavior has been obtained by computer simulations.

A completely different circuit with chaotic behavior has been proposed by Rodriguez-Vazquez, Huertas, and Chua [28]. It is a switched-capacitor circuit that directly implements the transformation (6.1).

VIII. Autonomous Circuits

The present paper concentrates mainly on nonautonomous circuits and we just mention a few examples of chaotic autonomous circuits.

The best known example is Chua's circuit, represented in Fig. 35, with the nonlinear resistor characteristic of Fig. 36 (cf. [29] and references therein, [30]-[32]). In [29], it is shown that this circuit, for certain parameter values, has a homoclinic orbit. By a theorem of Shilnikov [25], this implies "horseshoe chaos" in a neighborhood of these parameter values.

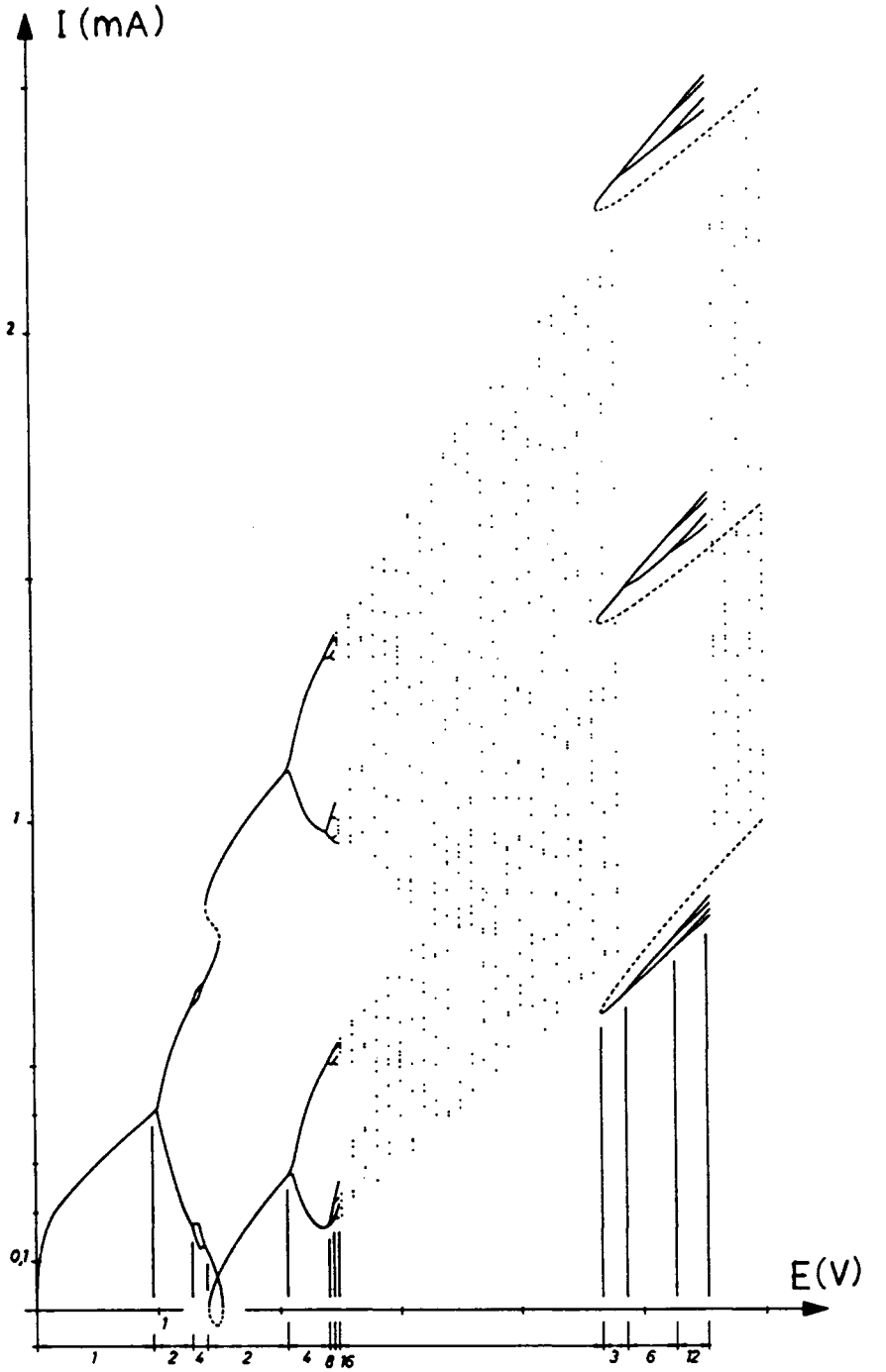

Fig. 32. Computed bifurcation diagram of the piecewise-linear *R-L*-diode circuit (from [20]).

Earlier experimental and computer simulation evidence for chaos in a third-order autonomous circuit has been presented by Freire, Franquelo, and Aracil [33]. Finally, we mention the circuit of Saito [34] where it was possible to prove chaotic behavior by elementary methods.

IX. Conclusion

We have discussed a certain number of circuits whose time evolutions have a chaotic asymptotic behavior, if the circuit parameters are chosen in suitable intervals. The "routes to chaos" through sequences of subharmonics have also been presented. In the rare cases, where rigorous mathematical arguments assure the presence of chaos, we have given an outline of them.

We are convinced that the engineer at large will eventually become aware of the fact that chaotic behavior may occur in electrical circuits. As a consequence, many new examples will pop up where chaos has been observed in real operating systems. Then there will be an urgent need

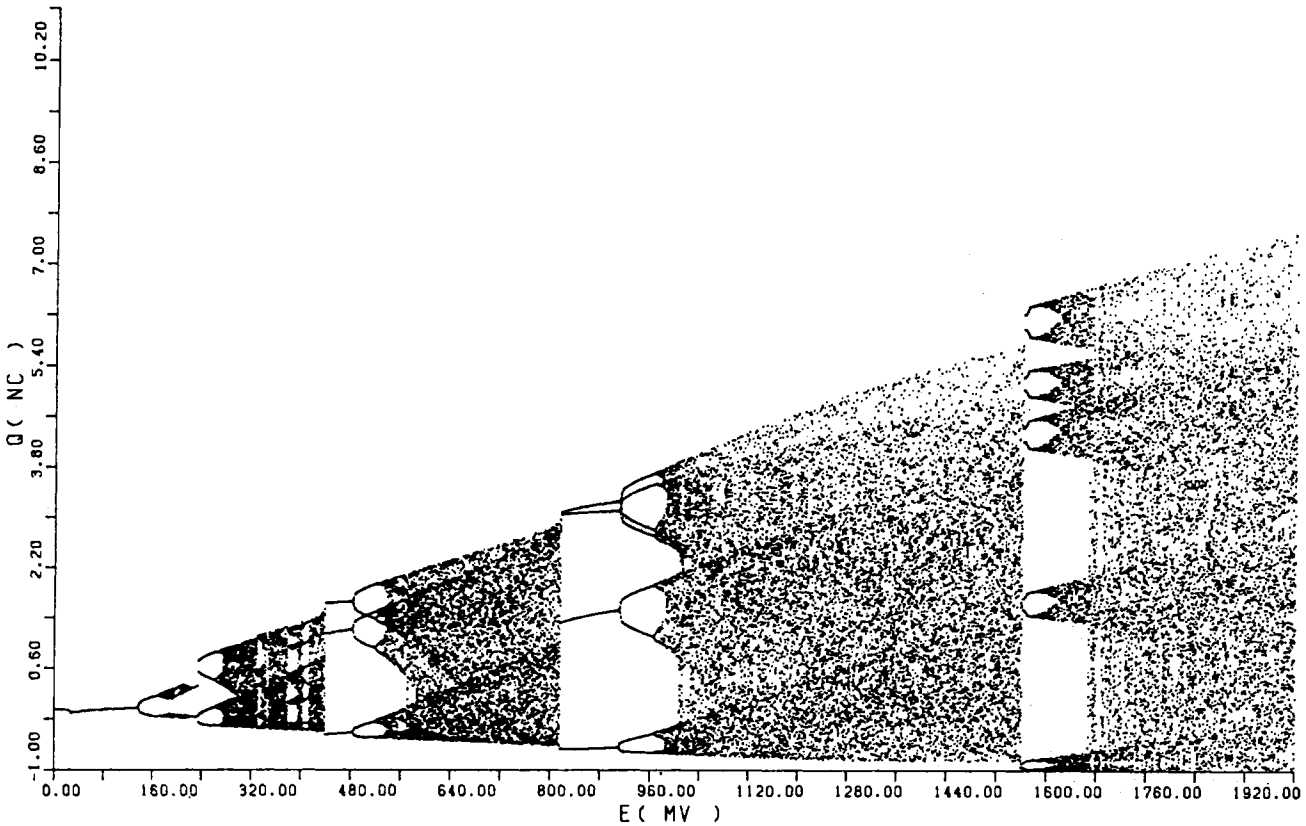

Fig. 33. Bifurcation diagram of the circuit without nonlinear resistor (from [21]).

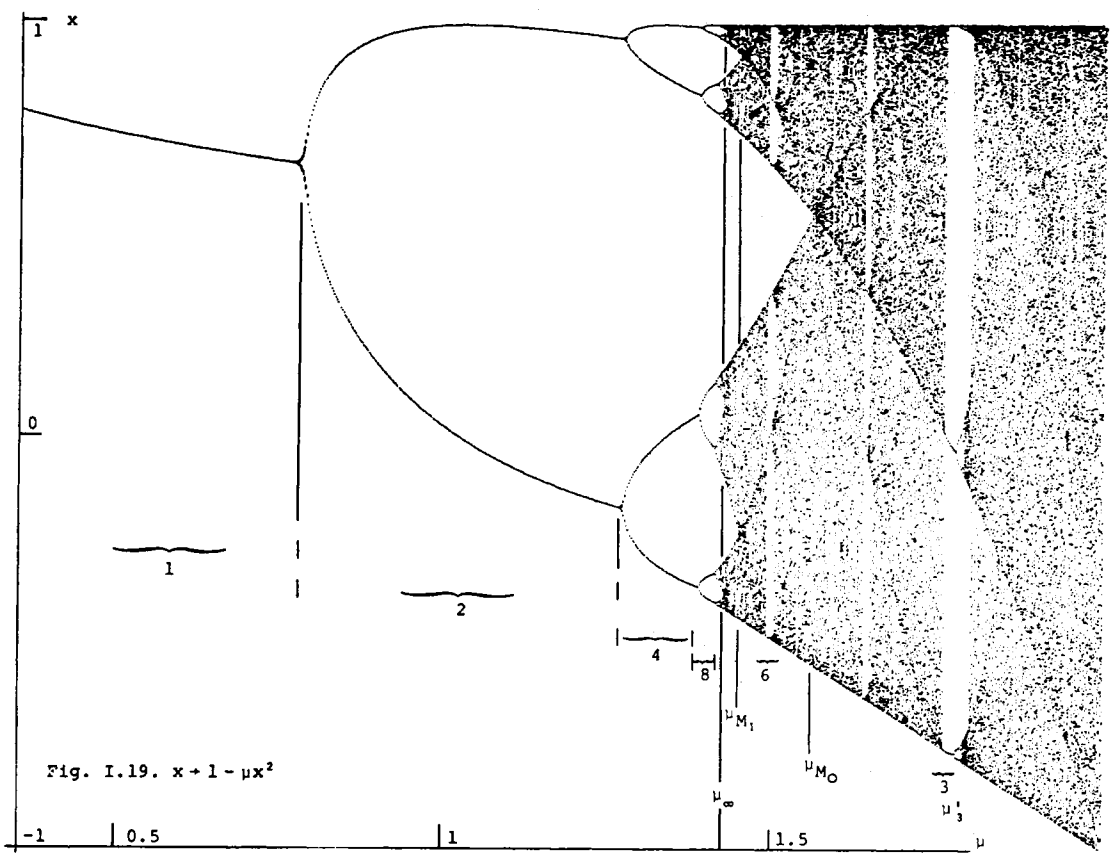

Fig. 34. Bifurcation diagram for the iterations of the function defined in (6.1) (from [22]).

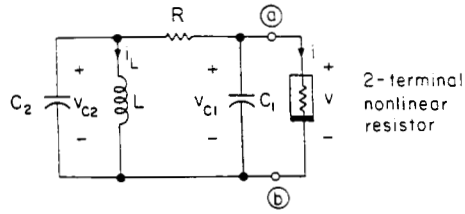

Fig. 35. Chua's circuit.

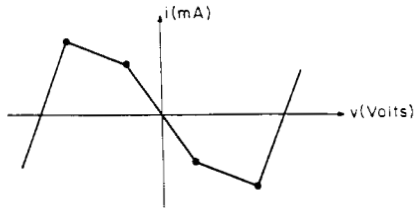

Fig. 36. Nonlinear resistor characteristic of Chua's circuit.

for a coherent theory that allows to foresee and eliminate this kind of malfunctioning.

References

[1] J. K. Hale, *Ordinary Differential Equation*. New York, NY: Wiley-Interscience, 1969.

[2] I. Gumowski and C. Mira, *Dynamique Chaotique* (Collection Nabla). Toulouse, France: Cepadues Editions, 1980.

[3] M. Hasler and J. Neirynck, *Nonlinear Circuits*. Boston, MA: Artech House, 1986.

[4] M. L. Cartwright and J. E. Littlewood, "On non-linear differential equation of the second order: I. The equation $y - k(1 - y^2)y = y = b\lambda k \cos(\lambda t + \alpha)$, k large," *J. London Math. Soc.*, vol. 20, pp. 180–189, 1945.

[5] J. E. Littlewood, "On non-linear differential equations of the second order: III. The equation $y - k(1 - y^2)y + y = b\lambda k \cos(\lambda t + \alpha)$, for large k, and its generalizations," *Acta Math.*, vol. 97, pp. 267–308, 1957.

[6] N. Levinson, "A second order differential equation with singular solutions," *Ann. Math.*, vol. 50, pp. 127–153, 1949.

[7] S. Smale, "Differentiable dynamical systems," *Bull. Amer. Math. Soc.*, vol. 73, pp. 747–817, 1967.

[8] M. Levi, "Qualitative analysis of the periodically forced relaxation oscillations," *Mem. Amer. Math. Soc.*, vol. 32, no. 244, 1981.

[9] T. S. Parker and L. O. Chua, "A computer-assisted study of forced relaxation oscillations," *IEEE Trans. Circuits Syst.*, vol. CAS-30, pp. 518–533, 1983.

[10] B. Van der Pol and J. Van der Mark, "Frequency demultiplication," *Nature*, vol. 120, pp. 363–364, 1927.

[11] M. P. Kennedy and L. O. Chua, Van der Pol and chaos," *IEEE Trans. Circuits Syst.*, vol. CAS-33, pp. 974–980, 1986.

[12] L.-Q. Pei, F. Guo, S.-X. Wu, and L. O. Chua, "Experimental confirmation of the period-adding route to chaos in a nonlinear circuit," *IEEE Trans. Circuits Syst.*, vol. CAS-33, pp. 438–442, 1986.

[13] L. O. Chua, Y. Yao, and Q. Yang, "Devil's staircase route to chaos in a non-linear circuit," *Int. J. Circuit Theory Appl.*, vol. 14, pp. 315–329, 1986.

[14] B. Mandelbrot, *The Fractal Geometry of Nature*. New York, NY: Freeman, 1983.

[15] Y. Ueda and N. Akamatsu, "Chaotically transitional phenomena in the forced negative-resistance oscillator," *IEEE Trans. Circuits Syst.*, vol. CAS-28, pp. 217–224, 1981.

[16] H. Kawakami and C. Hayashi, "Bifurcations and chaotic states of the solutions of the Duffing-Van der Pol equation," presented at the 26th Int. Scientific Colloquium, Illmenau Inst. Technol., 1981. Also in *Lectures in Electrical Engineering*, Illmenau Inst. Technol., Illmenau, East Germany, 1981.

[17] Y. S. Tang, A. I. Mees, and L. O. Chua, "Synchronization and chaos," *IEEE Trans. Circuits Syst.*, vol. CAS-30, pp. 620–626, 1983.

[18] J. Testa, J. Pérez, and C. Jeffries, "Evidence for universal chaotic behavior of a driven nonlinear oscillator," *Phys. Rev. Lett.*, vol. 48, pp. 714–717, 1982.

[19] A. Azzouz, R. Duhr, and M. Hasler, "Transition to chaos in a simple nonlinear circuit driven by a sinusoidal source," *IEEE Trans. Circuits Syst.*, vol. CAS-30, pp. 913–914, 1983.

[20] ——, "Bifurcation diagram for a piecewise linear circuit," *IEEE Trans. Circuits Syst.*, vol. CAS-31, pp. 587–588, 1984.

[21] T. Matsumoto, L. O. Chua, and S. Tanaka, "Simplest chaotic nonautonomous circuit," *Phys. Rev. A*, vol. 30, pp. 1155–1157, 1984.

[22] P. Collet and J.-P. Eckmann, *Iterated Maps on the Interval as Dynamical Systems*. Boston, MA: Birkhäuser, 1980.

[23] T.-H. Yoon, J.-W. Song, S.-Y. Shin, and J.-W. Ra, "One-dimensional map and its modification for periodic-chaotic sequence in a driven nonlinear oscillator," *Phys. Rev. A*, vol. 30, pp. 3347–3350, 1984.

[24] Y. Ueda, "Randomly transitional phenomena in the system governed by Duffings equation," *J. Stat. Phys.*, vol. 20, pp. 181–196, 1979.

[25] J. Guckenheimer and P. Holmes, *Nonlinear Oscillations, Dynamical Systems and Bifurcations of Vector Fields*. New York, NY: Springer, 1983.

[26] F. M. A. Salem and S. S. Sastry, "Dynamics of the forced Josephson junction circuit: The region of chaos," *IEEE Trans. Circuits Syst.*, vol. CAS-32, pp. 784–796, 1985.

[27] L. O. Chua, M. Hasler, J. Neirynck, and P. Verburgh, "Dynamics of a piecewise-linear resonant circuit," *IEEE Trans. Circuits Syst.*, vol. CAS-29, pp. 535–547, 1982.

[28] A. B. Rodriguez-Vazquez, J. L. Huertas, and L. O. Chua, "Chaos in a switched capacitor circuit," *IEEE Trans. Circuits Syst.*, vol. CAS-32, pp. 1083–1084, 1985.

[29] L. O. Chua, M. Komuro, and t. Matsumoto, "The double scroll family, parts I and II," *IEEE Trans. Circuits Syst.*, vol. CAS-33, pp. 1072–1118, Nov. 1986.

[30] M. J. Ogorzalek, "Chaotic regions from double scroll," *IEEE Trans. Circuits Syst.*, vol. CAS-34, pp. 201–203, Feb. 1987.

[31] M. E. Broucke, "One parameter bifurcation diagram for Chua's circuit," *IEEE Trans. Circuits Syst.*, vol. CAS-34, pp. 208–209, Feb. 1987.

[32] Lin Yang, Youlin Liao, "Self-similar bifurcation structures from Chua's circuit," to appear in *Int. J. Circuit Theory Appl.*

[33] E. Freire, L. G. Franquelo, and J. Aracil, "Periodicity and chaos in an autonomous electronic system," *IEEE Trans. Circuits Syst.*, vol. CAS-31, pp. 237–247, 1984.

[34] T. Saito, "A chaos generator based on a quasi-harmonic oscillator," *IEEE Trans. Circuits Syst.*, vol. CAS-32, pp. 320–331, 1985.

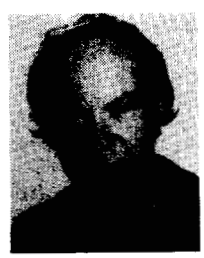

Martin J. Hasler (Member, IEEE) was born in Wetzikon, Switzerland, in 1945. He received the Diploma in 1969 and the Ph.D. degree in 1973 from the Swiss Federal Institute of Technology (ETH), Zurich, both in physics.

He continued research in mathematical physics as a Research Assistant at Bedford College, University of London, from 1973 to 1974. At the end of 1974 he joined the Circuit Theory group of the Swiss Federal Institute of Technology, Lausanne (EPFL), where he was given the title of a Professor in 1984. His research interests are in the field of nonlinear circuits. He is the coauthor, with J. Neirynck, of the books *Filtres Électrique*, 1981, and *Circuits Non Linéaires*, 1984, published in French by the Presses Polytechniques Romandes, Lausanne. The English translations *Electric Filters* and *Nonlinear Circuits* have both been published by Artech House, Boston, MA, in 1986.